

Supplementary Material for:

Negative coupling: the coincidence of premating isolating barriers
can reduce reproductive isolation

Thomas G. Aubier, Michael Kopp, Isaac J. Linn, Oscar Puebla,
Marina Rafajlović, Maria R. Servedio

Content:

Supplementary Figures S1 to S7

Figure S1. Comparison of equilibrium states with versus without P^B , with linkage between the preference and the trait loci (with recombination occurring at rate 0.1, assuming that gene order is $P^B P^A T^B$). We compare the equilibrium states with P^B versus without P^B , and represent the change in allelic divergence (**a-c**) and the change in normalized LD (**d-f**). See caption of fig. 3 for details (but note that the color scale is different here). In panel **a**, Roman numerals refer to the different regimes summarized in tab. 1, but note that they are not placed at the same locations (i.e., the same combinations of r_T and r_P) as in fig. 3 (hence the use of a pink background; see explanation below). Here, green pixels represent parameter combinations where genetic variation is lost at the T^A and T^B loci (loci P^A and P^B then become neutral). We obtain a similar outcome as with free recombination between the preference and the trait loci (fig. 3), except for the loss of genetic variation that occurs in the domain of regime **IIIa**, and the fact that primary effect (1) under regime **I** can occur alongside an increase in divergence at the T^B locus due to the presence of P^B (at the very top left of panel **c**). In particular, we observe that the same regimes, from **I** to **V** under which primary effects (1) to (5) prevail as summarized in tab. 1, occur as in the case of free recombination (fig. 3). Here, $s = 0.5$, $m_2 = 0.01$ and $\alpha = 5$.

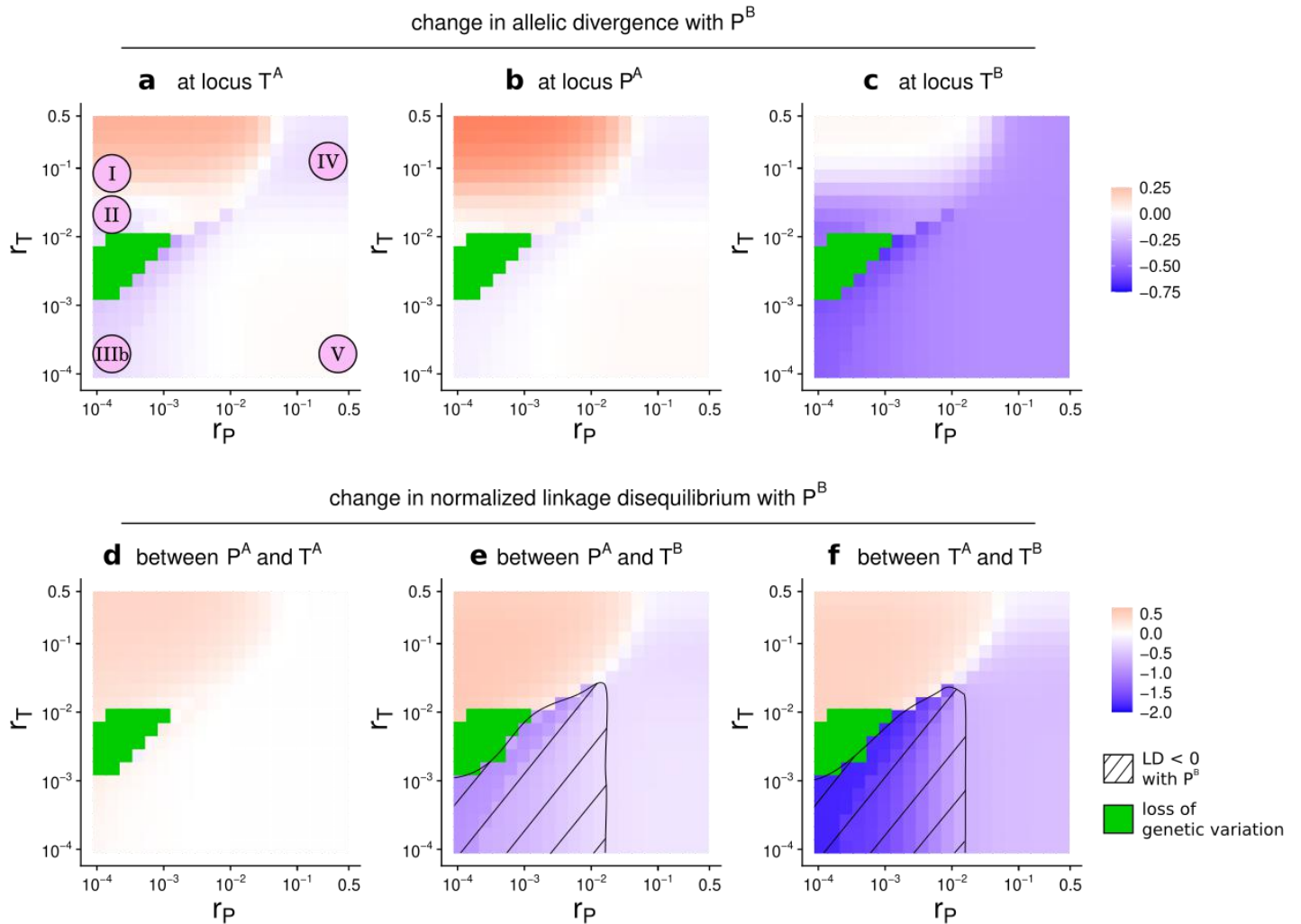


Figure S2. Comparison of equilibrium states with versus without P^B , with weak asymmetrical viability selection on T^A between populations ($s_1^A = 1.01s_2^A$). We compare the equilibrium states with P^B versus without P^B , and represent the change in allelic divergence (**a-c**) and the change in normalized LD (**d-f**). See caption of fig. 3 for details. Here, green pixels represent parameter combinations where genetic variation is lost at the T^A and T^B loci (loci P^A and P^B then become neutral). We obtain qualitatively the same outcome as without asymmetrical viability selection (fig. 3), except for the loss of genetic variation that occurs in the domain of regime **IIIa**. Here, $s_2^A = 0.5$, $m = 0.01$ and $\alpha = 5$.

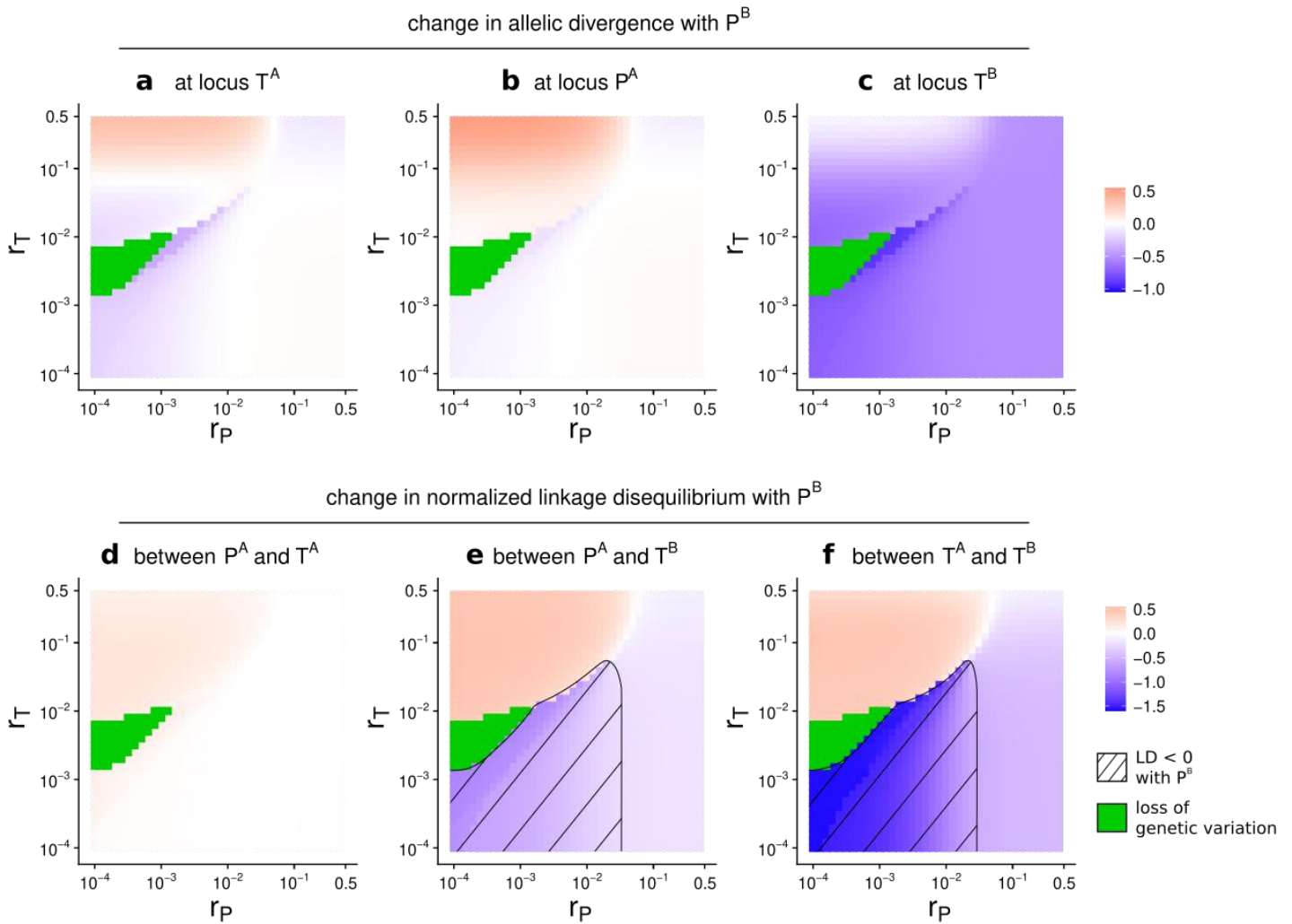


Figure S3. Comparison of equilibrium states with versus without P^B , with weak asymmetrical preference strength induced by P^A between populations ($\alpha_1^A = 1.01\alpha_2^A$). We compare the equilibrium states with P^B versus without P^B , and represent the change in allelic divergence (**a-c**) and the change in normalized LD (**d-f**). See caption of fig. 3 for details. Here, green pixels represent parameter combinations where genetic variation is lost at the T^A and T^B loci (loci P^A and P^B then become neutral). We obtain qualitatively the same outcome as without asymmetrical preference strength (fig. 3), except for the loss of genetic variation that occurs in the domain of regime **IIIa**. Here, $s = 0.5$, $m = 0.01$ and $\alpha_2^A = 5$.

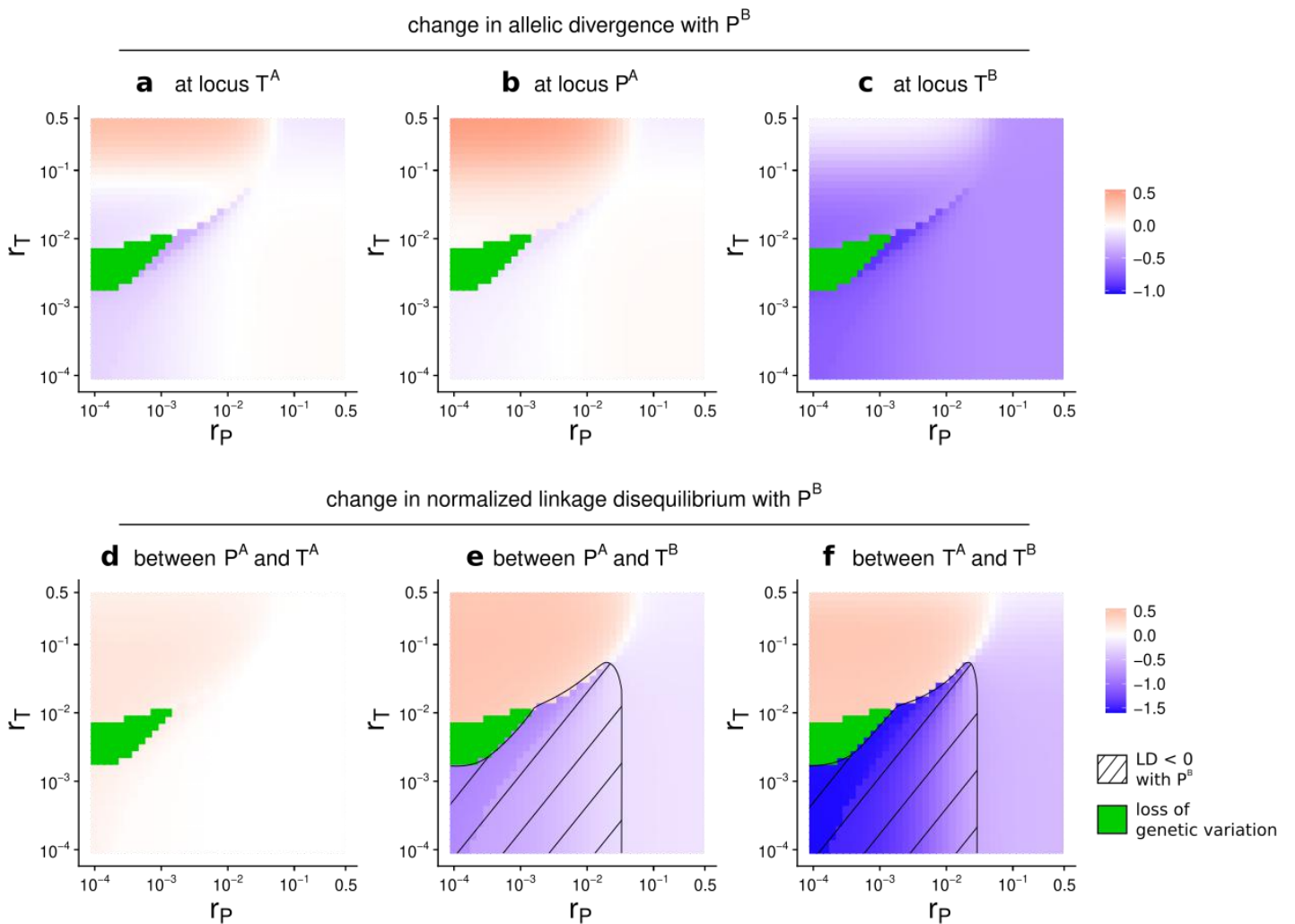


Figure S4. Comparison of equilibrium states with versus without P^B , with weak asymmetrical migration between populations ($m_1 = 1.01m_2$). We compare the equilibrium states with P^B versus without P^B , and represent the change in allelic divergence (**a-c**) and the change in normalized LD (**d-f**). See caption of fig. 3 for details. We obtain qualitatively the same outcome as without asymmetrical migration (fig. 3). Here, $s = 0.5$, $m_2 = 0.01$ and $\alpha = 5$.

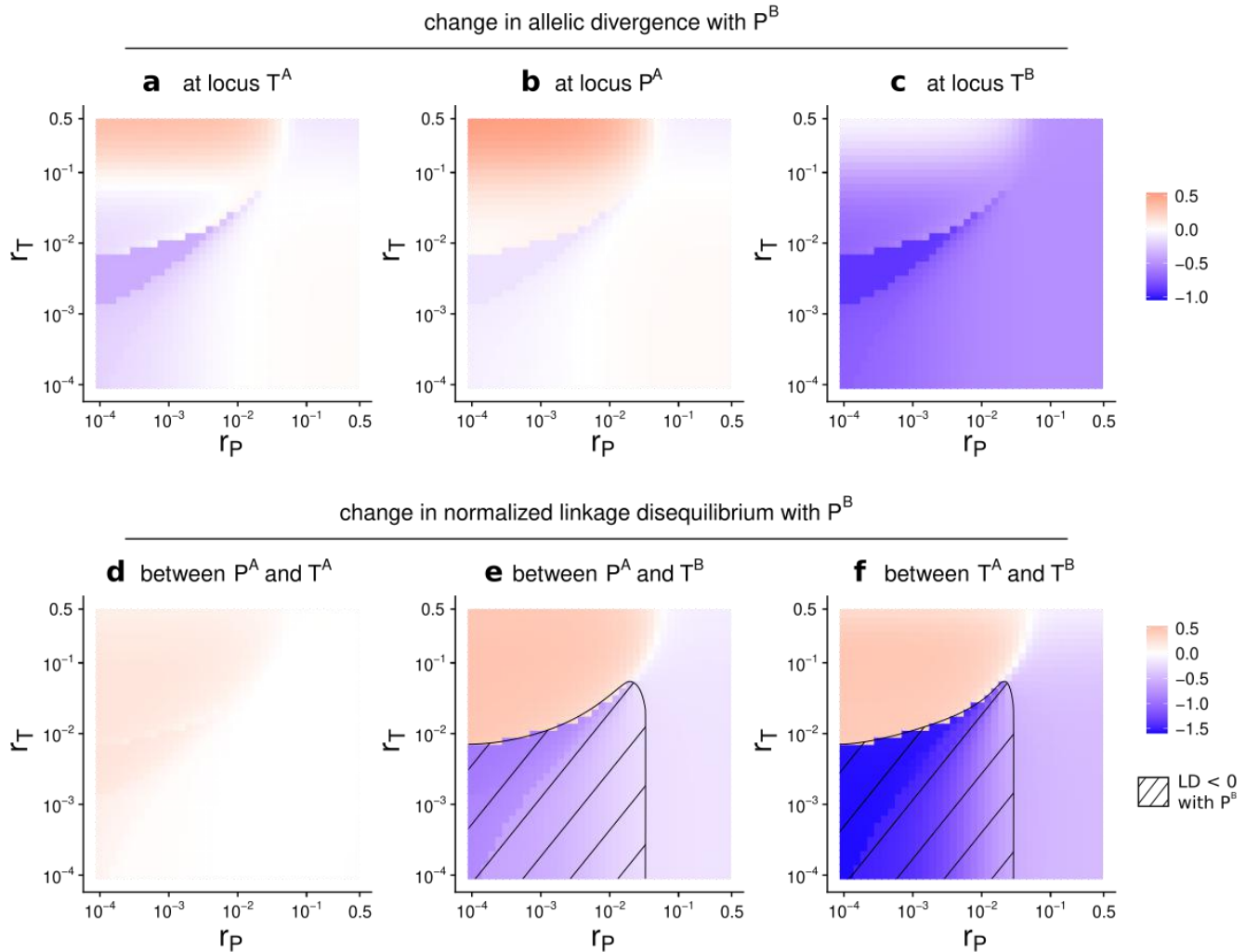


Figure S5. Comparison of equilibrium states with versus without P^B , with weaker viability selection and choosiness ($s = 0.05$; $\alpha = 1$). We compare the equilibrium states with P^B versus without P^B , and represent the change in allelic divergence (**a-c**) and the change in normalized LD (**d-f**). See caption of fig. 3 for details (but note that the color scale is different here). In panel **a**, Roman numerals refer to the different regimes summarized in tab. 1, but note that they are not placed at the same locations (i.e., the same combinations of r_T and r_P) as in fig. 3 (hence the use of a pink background; see explanation below). Here, green pixels represent parameter combinations where genetic variation is lost at the T^A and T^B loci (loci P^A and P^B then become neutral). We obtain a similar outcome as with strong viability selection and choosiness (fig. 3), except for the loss of genetic variation that occurs here, and the absence of regime **V**. In particular, we observe that the same regimes (from **I** to **IV**) under which primary effects (1) to (4) prevail as summarized in tab. 1, occur as in the case of strong viability selection and choosiness (fig. 3). With such low viability selection ($s = 0.05$) but with stronger choosiness (e.g. $\alpha = 5$), a loss of genetic variation occurs for most recombination rates, due to the homogenizing effect of sexual selection that is not overcome by divergent viability selection (not shown). Here, $m = 0.01$.

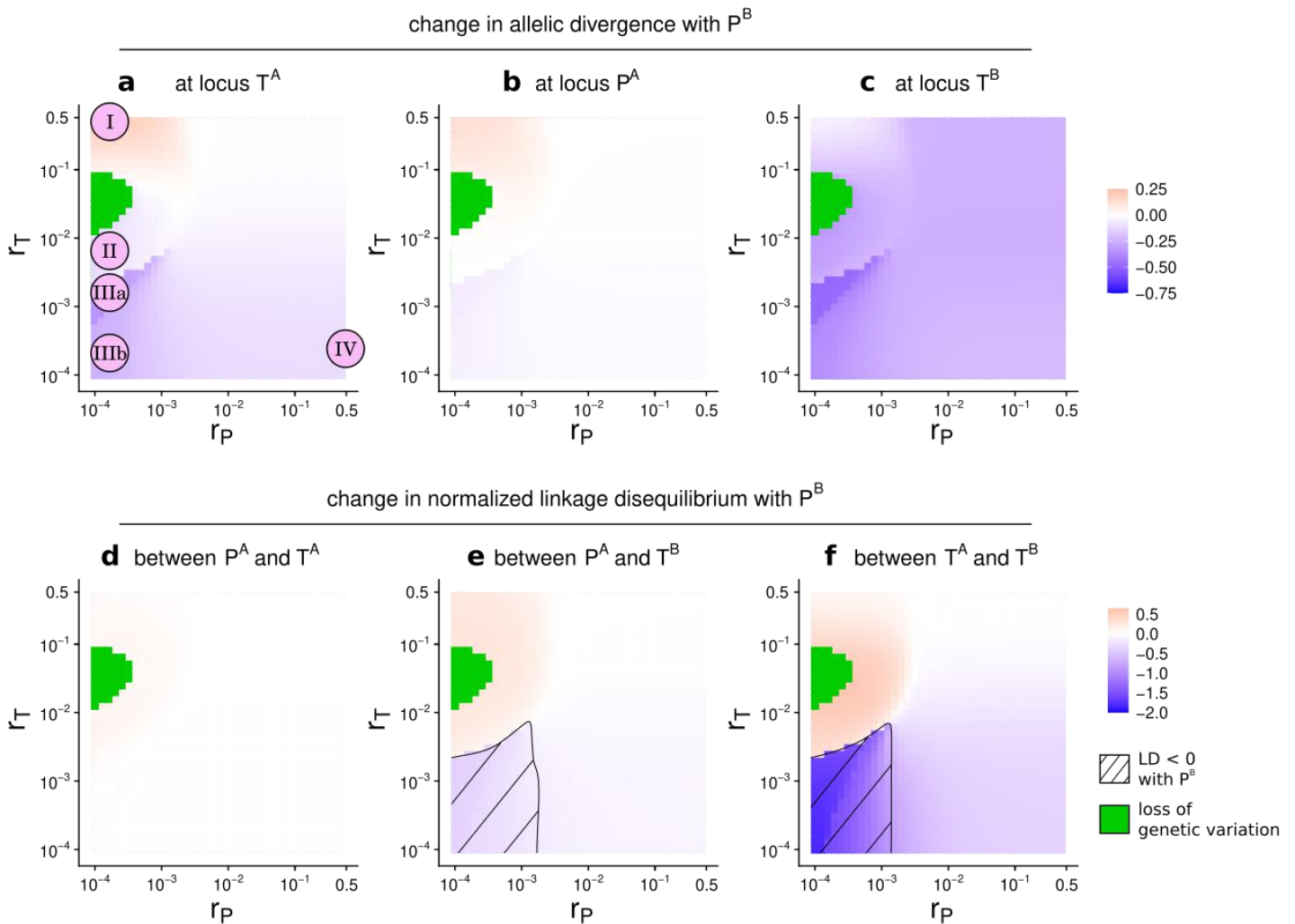


Figure S6. Comparison of equilibrium states with versus without P^B , with viability selection acting in both sexes and with weaker viability selection and choosiness ($s = 0.05$; $\alpha = 1$). We compare the equilibrium states with P^B versus without P^B , and represent the change in allelic divergence (**a-c**) and the change in normalized LD (**d-f**). See caption of fig. 3 for details (but note that the color scale is different here). In panel **a**, Roman numerals refer to the different regimes summarized in tab. 1, but note that they are not placed at the same locations (i.e., the same combinations of r_T and r_P) as in fig. 3 (hence the use of a pink background; see explanation below). Here, green pixels represent parameter combinations where genetic variation is lost at the T^A and T^B loci (loci P^A and P^B then become neutral). We obtain a similar outcome as with viability selection acting in males only (fig. S5), except for the loss of genetic variation, which occurs for a large set of recombination rates, and for the absence of regime **V**. In particular, we observe that the same regimes, from **I** to **IV** under which primary effects (1) to (4) prevail as summarized in tab. 1, occur as in the case of viability selection acting in males only (fig. S5). With stronger viability selection and choosiness (e.g. $s = 0.5$ and $\alpha = 5$, as in fig. 3), genetic divergence is very strong when viability selection acts in both sexes, and changes in divergence due to the presence of P^B are often negligible (not shown). We note, however, that regime **II** is absent when choosiness is strong enough (e.g. for $\alpha = 5$, for $s = 0.05$ or $s = 0.5$; not shown). Here, $m = 0.01$.

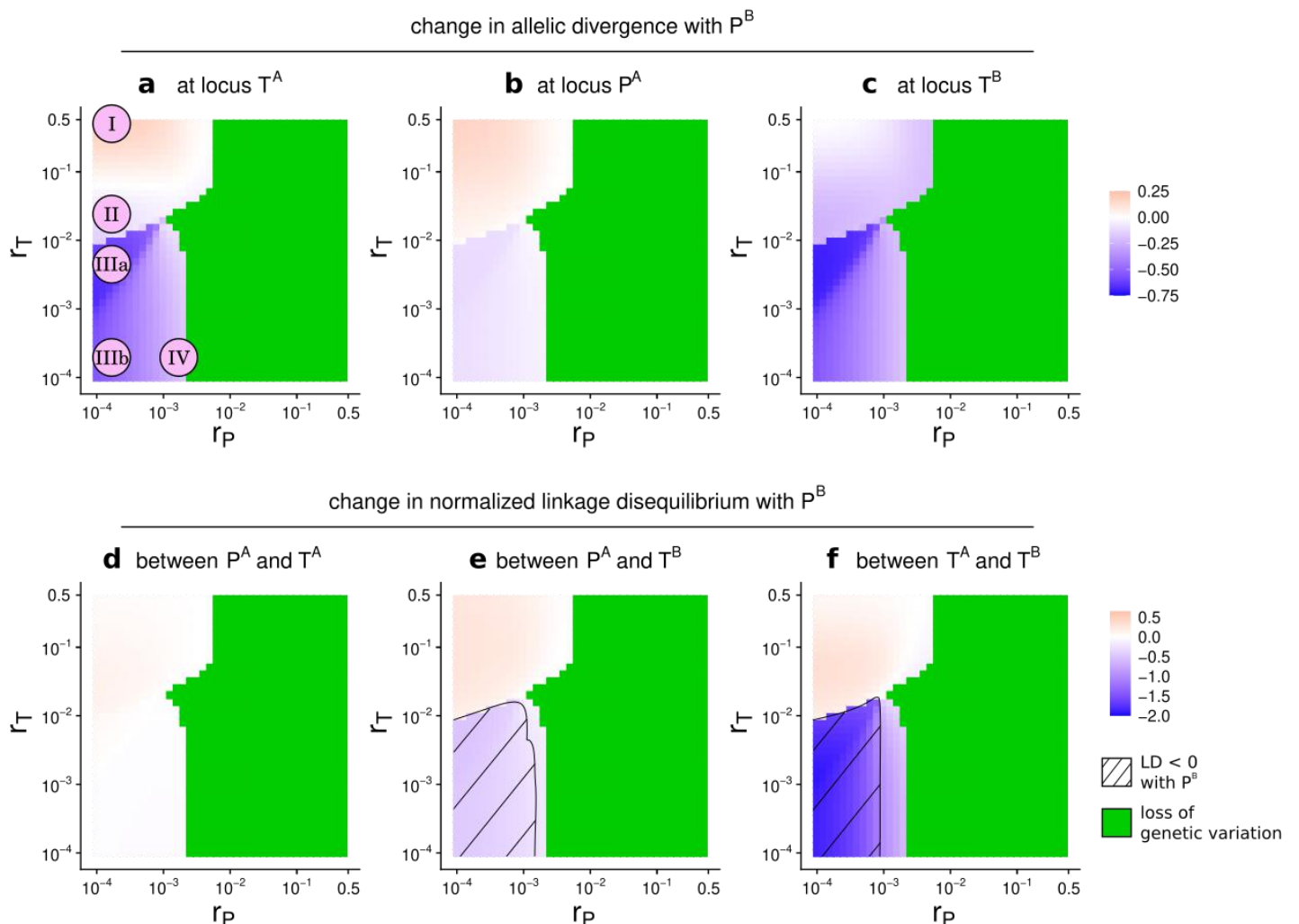


Figure S7. Comparison of equilibrium states with versus without P^B , with an alternate gene order $P^A T^A T^B P^B$. Here, recombination occurs at a rate r_{TT} between the trait loci T^A and T^B , and at a rate r_{PT} between the loci within each preference-trait set (both between loci P^A and T^A , and between loci P^B and T^B). We compare the equilibrium states with P^B versus without P^B , and represent the change in allelic divergence (**a-c**), the change in normalized LD (**d-f**), and the change in reproductive isolation (RI; **g**). See caption of figs. 2 and 4 for details. For the parameter combination tested, negative coupling occurs when recombination occurs at a lower rate within a set than between sets (for $r_{PT} > r_{TT}$, which corresponds to the case where the presence of many “recombinant” females with “mismatched” preferences increase the mating success of “recombinant” males with “mismatched” traits, as in our main analysis; **g**). This occurs through a decreased LD between the T^A and T^B loci, albeit without the establishment of negative LD between the P^A and P^B loci (**f**; primary effect (4) in tab. 1). Further theoretical studies are needed to understand how gene order determines the outcome in terms of coupling. Note that for $r_{PT} = 0.5$, we obtain the same outcome as in our main analysis for $r_P = 0.5$ (fig. 2), as in both cases, only the trait loci are physically linked with each other. Here, $s = 0.5$, $m = 0.01$ and $\alpha = 5$.

